ADVANCED ELECTRONIC MATERIALS
www.advelectronicmat.de

Topological Structures in Multiferroics – Domain Walls, Skyrmions and Vortices

Jan Seidel, Rama K. Vasudevan, and Nagarajan Valanoor**

Topological structures in multiferroic materials have recently received considerable attention because of their potential use as nanoscale functional elements. Their reduced size in conjunction with exotic arrangement of the ferroic order parameter and potential order parameter coupling allows for emergent and unexplored phenomena in condensed matter and functional materials systems. This will lead to exciting new fundamental discoveries as well as application concepts that exploit their response to external stimuli such as mechanical strain, electric and magnetic fields. In this review we capture the current development of this rapidly moving field with specific emphasis on key achievements that have cast light on how such topological structures in multiferroic materials systems can be exploited for use in complex oxide nanoelectronics and spintronics.

1. Introduction

Topological defects play important roles in nature. They are found in fields as diverse as cosmology,[1] particle physics, superfluidity, liquid crystals, and metallurgy, manifesting themselves as e.g. screw/edge-dislocations in liquid crystals,[2] magnetic flux tubes in superconductors,[3] and vortices in superfluids[4] etc.

The theory of topological defects, as applicable to condensed matter physics, dates back to the seminal work of Mermin in 1979.[5] In a non-uniform ordered medium (i.e., media that can be described by a function f(**r**) which assigns an order parameter to every point in that space), topological defects are those regions including points, lines and surfaces where the order parameter ceases to vary continuously, forming regions of lower dimensionality. At the same time, the possible values that the order parameter can take constitute the order parameter space. For example, the order parameter space for planar spins can be taken as a unit vector that can point in any direction in a plane, i.e., the space is a circle. This allows for mapping of a closed contour of the order parameter from real space to the order parameter space, and leading to a definition of the winding number *(*integer *n)*, which determines the number of times that this mapping wraps the closed curve around the circle in the order parameter space. For example, uniform spins map to a single point on the circle, and therefore produce a winding number of zero, whereas concentric rings clearly wrap the order parameter space once, leading to $n = 1$. Note that here, 1 stipulates counter-clockwise, and -1 clockwise. These theories are important to understand why, for example, annihilation of topological defects occurs when defects with opposite winding numbers approach each other, as well as dislocations and disclinations, etc., although the reader is referred to the original Mermin work for more detail.[5]

In condensed matter systems, topological structures are inherent to ferroic materials, i.e. materials with a spontaneous reversible ordering, such as magnetic materials, ferroelectrics and ferroelastic materials. Ferroics are used widely in sensors, actuators, information technology and other smart materials applications.[6,7] Due to degeneracy in possible orientations of the order parameter upon cooling below the ferroic phase transition temperature, ferroic phases tend towards the formation of discrete domain structures. Adjacent domains are separated by naturally occurring planar topological defects called domain walls. Over the last few years they have been intensively investigated with respect to their inherent functional behavior in various studies involving ceramics, thin films and single crystalline material. The fact that the electronic conductivity of domain walls in ferroelectrics and multiferroics can be utilized for nanoscale functional elements[8,9] has spawned world-wide interest in exploiting novel domain wall-driven concepts in memory and spintronic applications. This has consequently led to the finding of unique properties associated with such topological structures. The understanding of these phenomena has progressed to a point where we can say that the physical properties of topological structures such as domain walls can be completely different from those of the parent bulk material phase.[10] Similar considerations regarding electronic conductivity apply to structural phase boundaries,[11–13] which might for example occur in materials exhibiting morphotropic phase boundaries, which includes multiferroic $BiFeO_3$ (BFO).[14]

Although domain walls are the commonly understood concept of ferroic order, they are not the only way in which spatially

Prof. J. Seidel, Prof. N. Valanoor
School of Materials Science and Engineering
UNSW Australia
Sydney, Australia
E-mail: jan.seidel@unsw.edu.au;
nagarajan@unsw.edu.au
Dr. R. K. Vasudevan
Center for Nanophase Materials Sciences
and Institute for Functional Imaging of Materials
Oak Ridge National Laboratory
Oak Ridge, TN 37831

DOI: 10.1002/aelm.201500292

varying order parameters can be arranged. Alternatively, more complex patterns can develop in which the order parameter changes in different ways as described for example by the topological theory of defects in ordered media by Mermin.[5] When combined with local defects or singularities, the number of possible geometrical patterns that arise can be numerous, including vortex structures and skyrmions (see **Figure 1**). Which kind of ferroic micro- or nanostructure develops depends critically on the relative magnitudes of various energies associated with exchange, crystallographic anisotropy and adjacent surfaces. The physical dimensions of the specific material and its morphology are also important in determining the exact nature of the ferroic patterns that develop in equilibrium, which include flux-closure structures and other complex topological patterns such as periodic arrays of magnetic skyrmions, that can be observed by magnetic force microscopy.[15] Indeed, much of the initial excitement in ferroics with non-typical domain structures was spawned by ab initio calculations published in *Nature* by Naumov et al.,[16] who predicted the emergence of a new ferro-toroidic order parameter in nanodots of a ferroelectric material, although the observation of such states has remained elusive. Nevertheless, manipulation and control of the physical properties of other topological structures has resulted in a fertile and rich playground for research.

An interesting example was shown by Spaldin et al.[17] where the authors discuss how scaling behavior analysis of the Kibble-Zurek theory of topological defect formation (one of the core principles used to describe topological defect evolution in cosmology) can be applied to the hexagonal manganites. They propose the family of multiferroic hexagonal magnanites, $RMnO_3$ (R = Sc, Y, Dy to Lu) as a model system for testing the Kibble-Zurek mechanism. Generally, the study and manipulation of topological defects in ferroics offers a novel nanoelectronics characterization platform for future nanotechnologies.[18]

In this review, we have tried to cover recent advances and breakthroughs that have shaped the burgeoning field. Note that for length, this review is limited to multiferroic materials. Recent advances in domain wall manipulation and device engineering in traditional ferroelectrics such as $Pb(Zr,Ti)O_3$ (PZT) are not discussed. The reader is referred to other reviews on these topics.[19,20]

2. Local Structure Investigations of Multiferroic Domain Walls

The rapid developments made in high-resolution transmission electron microscopy (HRTEM) and scanning probe microscopy (SPM) have made it possible now to not only image topological defects but also perform functional measurements at their length scale. Whilst the existence of topological effects has been known for a while, it is only the giant leaps and bounds made in these microscopy techniques in recent years that have afforded direct evidence of the functional nature of topological defects.[21–28] In combination these allow for spatial mapping of functional properties with atomic (or near-atomic) precision. We briefly outline two successful methods in HRTEM that have greatly contributed to the development of domain imaging in multiferroics. First is the technique of exit wave reconstruction, pioneered at Juelich by Jia et al.[22] In 2007 Jia et al first

Jan Seidel is an Associate Professor at the School of Materials Science and Engineering at UNSW Australia. He received his doctorate in physics from the University of Technology Dresden in 2005. From 2006 to 2007, he was a Feodor Lynen Fellow (Alexander von Humboldt Foundation) at the University of California, Berkeley. From 2008 to 2011, he worked at Lawrence Berkeley National Laboratory. His main interests are in materials physics of complex oxide materials, especially fundamental electronic, optical and magnetic properties of interfaces and topological structures.

Rama K. Vasudevan is a postdoctoral researcher supervised by Prof. Sergei Kalinin at the Center for Nanophase Materials Sciences, Oak Ridge National Laboratory. He was awarded his PhD at UNSW in 2013 under the supervision of Prof. Nagarajan Valanoor, submitting a UNSW Faculty award-winning thesis on scanning probe microscopy of nanoscale ferroelectrics. His recent research interests include in-situ scanning tunneling microscopy of manganite thin films, as well as the use of big-data multivariate statistical analysis to understand complex oxides at mesoscopic and atomic scales.

Nagarajan (Nagy) Valanoor received his B. Engg in Metallurgy from the University of Pune (1997) and Ph.D from the University of Maryland (2001) under supervision of Prof. Ramesh in Materials Science and Engineering respectively. Following his PhD he continued as a research associate at Maryland until 2003. He followed this with a Alexander von Humboldt Fellowship with Prof. Rianer Waser at Forschungszentrum Juliech. In 2005 he was offered a lectureship at the School of Materials Science and Engineering, where he is currently Professor and Research Director. His research interests include understanding nanoscale phenemena in functional oxide interfaces and the synthesis of novel interfaces based on these understandings.

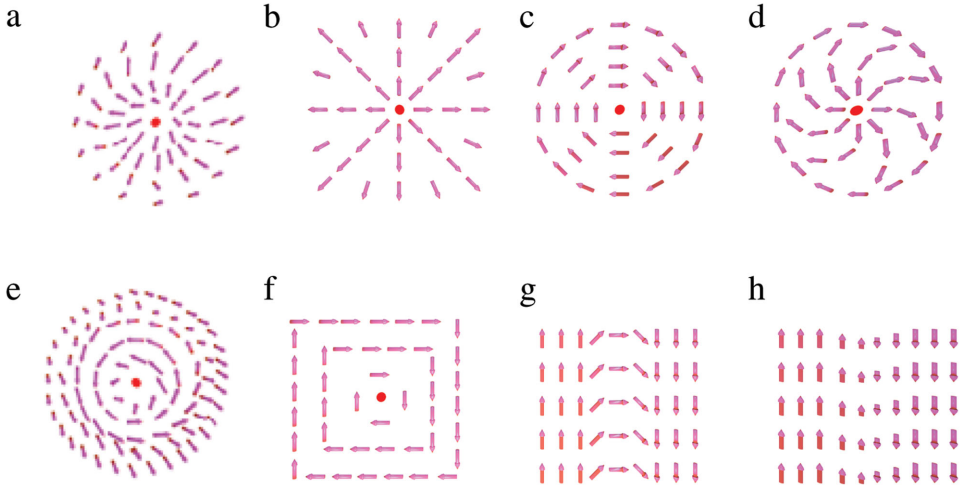

Figure 1. Examples of Topological Structures. Order parameter represented as arrows, 2D projection. a) Radial skyrmion, b–d) vortex structures, e) chiral skyrmion, f) four-quadrant closure structure. Structures (b–d) possess winding number of +1. Two types of domain walls are shown in (g) and (h), with a freely rotating order parameter in (g), and a steadily decreasing in magnitude (but fixed direction) vector in (h). Disclination centers are shown as red spheres.

showed direct quantification of the distortion in the lattice due to a spontaneous-polarization induced displacement.[29] Jia and colleagues thus have completely changed the landscape in which HRTEM is considered. No longer is it just a structural characterization technique – it offers the possibility of imaging the local polarization dipoles at atomic resolution, thus quantitatively measuring the local polarization and investigating the domain structure.[30] In this method the effects of objective-lens spherical aberration are corrected such that the image can be considered as true projection of the atomic columns. As a result, the continuous deviation across the topological defect (in this case a domain wall) can be mapped as shown in **Figure 2**.[31]

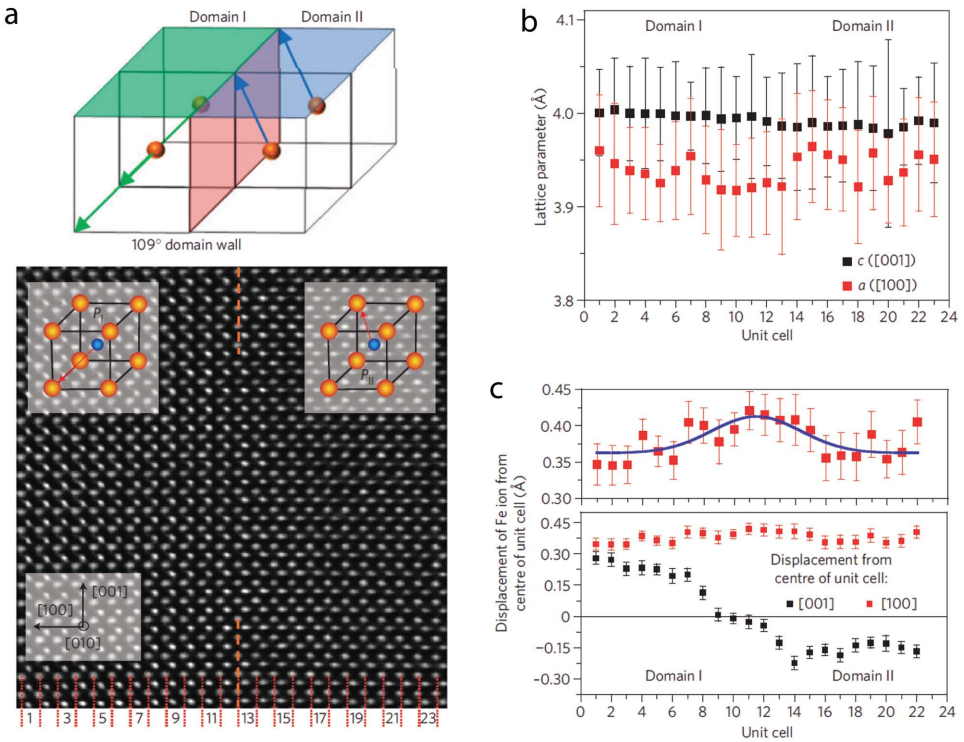

Figure 2. Structural analysis of domain walls in multiferroic bismuth ferrite. a) Schematic diagram of 109° domain wall and exit-wave-reconstructed HRTEM image of a 109° domain wall imaged along the [010] zone axis. b) Extracted *a* and *c* lattice parameters for each unit cell across the domain wall. c) Extracted Fe-ion displacement relative to the Bi lattice for each unit cell across the domain wall. A close-up (upper panel) reveals an increase in the component of polarization perpendicular to the domain wall. Reproduced with permission.[31] Copyright 2009, Nature Publishing Group.

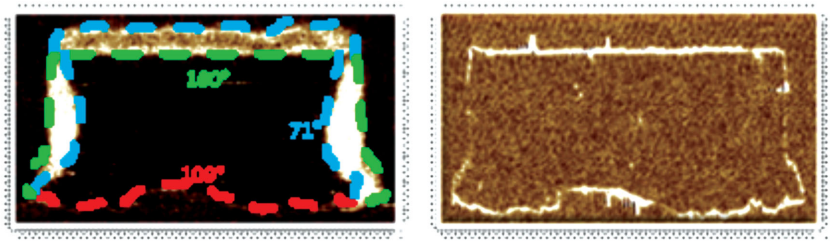

Figure 3. The three different types of domain walls in rhombohedral bismuth ferrite as seen in an in-plane PFM image of a written domain pattern in a mono-domain BFO (110) thin film (left) and the corresponding c-AFM image showing conduction at both 109° and 180° domain walls (right). Adapted with permission.[31] Copyright 2009, Nature Publishing Group.

An alternate approach is the so called weak beam transmission electron microscopy (WBTEM) technique. WBTEM makes it possible to perform quantitative analysis of the thickness fringes that appear on weak beam images of inclined domain walls. Fitting simulated fringe profiles to experimental ones gives the thickness of multiferroic domain walls.

Furthermore aberration corrected scanning TEM studies have also been able to map how the polarization vector varies around a dislocation core.[24] This is a fascinating example of how a structural topological defect (the dislocation) is intimately linked with the order parameter (polarization). Elemental and electronic structure analysis by electron-energy-loss spectroscopy (EELS) has also been applied to the study of domain walls.[32–34]

Nevertheless one must always bear in mind that TEM samples are very thin (typically a few tens of nm). We do not know yet how the mechanical and local electrostatic boundary conditions affect surface pinning of the domain walls. Although current state-of-the-art techniques permit atomic scale resolution at 0.5Å, the atomic displacements across a typical wall are on the order of 0.02 nm. This means direct imaging and interpretation must still not be subject to over-interpretation.

3. Conductivity at Multiferroic Domain Walls

It could be stated without reservation that the many variants of SPM (e.g. conductive atomic force microscopy – c-AFM, piezoresponse force microscopy – PFM) play a large and crucial role in the direct manipulation and characterization of topological defect structures on the nanoscale, including multiferroic domain walls.[35] The proximal probe nature of c-AFM means it can probe local conductivity at interfaces and topological defects without destroying the sample. In the same vein PFM has been further developed to include dynamic characterization of the switching process utilizing developments such as stroboscopic PFM and PFM spectroscopy, and has included for example instances of studying the effect of a single wall on switching[36] and nonlinear piezoelectric[37] dynamics.[38–41]

Domain wall conductivity has garnered immense interest from a functional perspective due potential non-volatile memory applications and electroresistive memory devices.[42] The presence of extended defects and oxygen vacancy accumulation has also been shown to influence transport and nucleation mechanisms at domain walls.[31,43,44] SPM techniques are one of the few techniques that allow us to gain local access to the processes that underpin the phenomena above. For example, the combination of local electromechanical and conductivity measurements revealed a connection between local current and pinning at bicrystal grain boundaries in bismuth ferrite.[45] This is mirrored in excitement by recent advances in the SPM-based characterization of ionic transport (for example oxygen) as well as oxygen vacancy movement in materials such as battery materials and electrodes.[46–49] The presence of extended defects and oxygen vacancies indeed can convolute the SPM signal which makes the identification of polarization mediated transport mechanisms difficult.

These advances in c-AFM and PFM are complemented by scanning tunnelling microscopy (STM) based measurements. STM can be used to probe directly the electronic structure at nanometer length scales; however it works only for conducting samples. In other words high-quality ferroelectric films with very low resistive leakage were typically not optimal for STM-based measurements. However the recent emergence of combined AFM/STM or SEM/STM systems have made it possible to map the electronic properties of domain walls in semi-insulating ferroelectric materials and heterostructures. Investigations using such combined tools have been demonstrated and include measurements on BFO domain walls.[50–53]

3.1. Origins of Domain Wall Conductivity

The changes in structure (and as a consequence electronic structure) that occurs at ferroelectric (multiferroic) domain walls[33] can lead to changes in transport behaviour (**Figure 3**). It is interesting that the original predictions of conduction at charged ferroelectric domain walls date back to Guro et al.,[54] where it was argued that the charge at the wall would result in accumulation or depletion of carriers, leading to large changes in carrier concentration and subsequent change in conductivity. Indeed, domain wall conductivity itself is shown to have varying transport behaviour and origins depending on the multiferroic in which the wall exists and the detailed synthesis method used to grow the materials. The domain walls of BFO were found to be more conductive than the domains,[55,56] On the other hand those in $YMnO_3$ were found to be more insulating or conductive depending on their orientation (see **Figure 4**).[57,58] We highlight that the ferroelectricity itself is fundamentally different between these two well-studied multiferroic candidates.

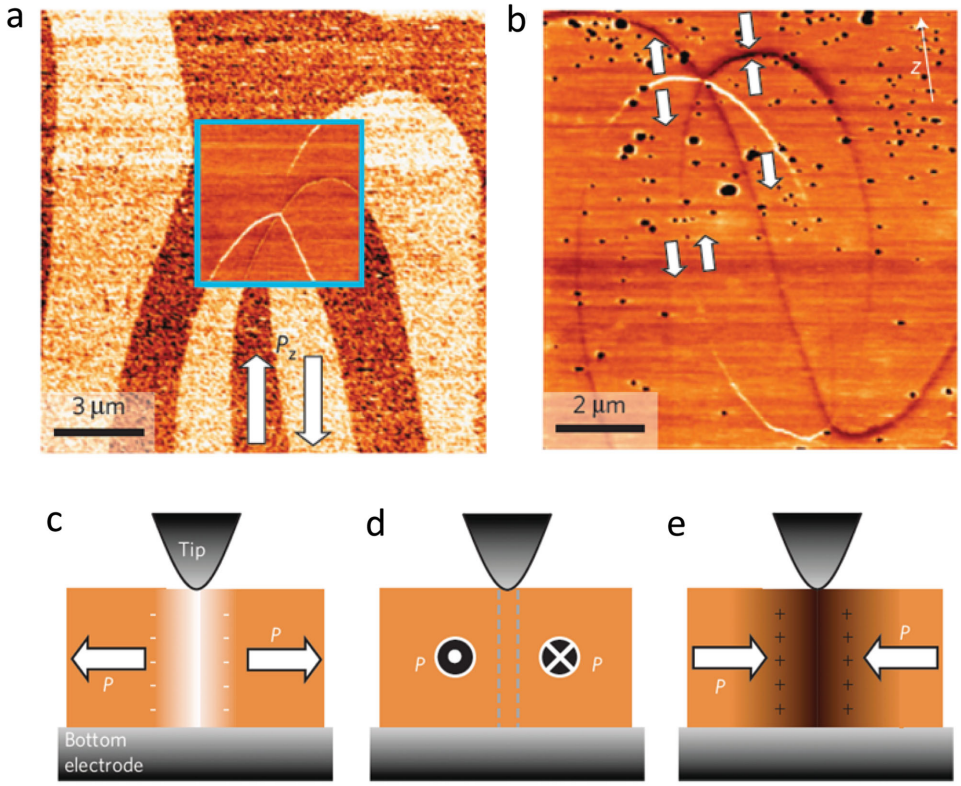

Figure 4. Anisotropic electrical conductance of charged improper ferroelectric domain walls. a) PFM image obtained in the yz-plane of an $ErMnO_3$ crystal. Arrows indicate the direction of polarization. The inset shows a c-AFM image acquired at the same position. Domain walls appear as lines of different brightness on an otherwise homogeneous background, reflecting their different conductance. b) c-AFM image of two neighbouring singularities in the yz-plane of $ErMnO_3$ with polarization directions in-plane as indicated. c–d) Schematic illustrations showing tail-to-tail, side-by-side and head-to-head domain walls, respectively. A colour scale is used to represent the electrical conductance and the associated hole density (white, high; dark brown, low). Reproduced with permission.[58] Copyright 2012, Nature Publishing Group.

Multiferroic $YMnO_3$ is a so-called improper ferroelectric, in which ferroelectricity is not the primary order parameter but rather induced by structural trimerization coexisting with magnetism. Here, the domain walls are found to be charged and stable and their conductivity depends on the specific orientation of the domain wall with respect to the polarization vector.

One considered contribution to domain wall conductivity is that the domain wall itself has a lower band gap. Density functional theory (DFT) investigations by Lubk et al. and others investigated theoretically the electronic structure of domain walls in bismuth ferrite[59–61] These computational models find that the domain walls have a significantly reduced band gap compared to the *R*3*c* bulk structure. At the walls the lattice changes to approach the ideal cubic structure, in which the 180° Fe–O–Fe bond angle maximize the Fe 3*d*–O 2*p* hybridization and hence the bandwidth of the material. Note that in no case does the band gap approach zero in the wall region.[31] In addition, the same DFT calculations also revealed steps in the electrostatic potential for all domain wall types. Such steps which are correlated with (and caused by) small changes in the component of the polarization normal to the wall, also contribute to the electronic conductivity.[62] These changes in normal polarization are a consequence of the specific rotation of the polar vector across the domain wall, and are also found in other materials.[63] More recently, Bellaiche et al. show how that strain-engineering of domain wall functionalities can be exploited.[64]

A second factor that may contribute to domain wall conductivity is the flexoelectric coupling and inhomogeneous strain across the domain walls. Thermodynamic theory by Morozovska and colleagues has been used to investigate charged and uncharged domain walls in both uniaxial and multiaxial multoferroics.[65–67] They show that in uncharged domain walls for the case of BFO the flexoelectric coupling between the two varying order parameter drives the formation of the electrostatic potential step at the domain wall, whilst the change in bandgap is due to the deformation potential from inhomogeneous strain variations across the interface. They also show angle-dependency of the flexoelectric and electrostrictive mechanisms in circular domains of BFO. This was observed experimentally by Vasudevan et al.[68] where they show a dependence of conductivity of domain walls in BFO not only on orientation but also on curvature of the wall. In this work the authors image domain walls that are curved and likely charged, see **Figure 5**. A modulation of current, greater than 200% was achieved through I–V measurements along a charged, curved domain wall, while a variation of 500% was observed in c-AFM measurements in UHV conditions. These results were explained by Morozovska et al. as the effect of an anisotropic elastic strain leading to anisotropic polarization rotations at the

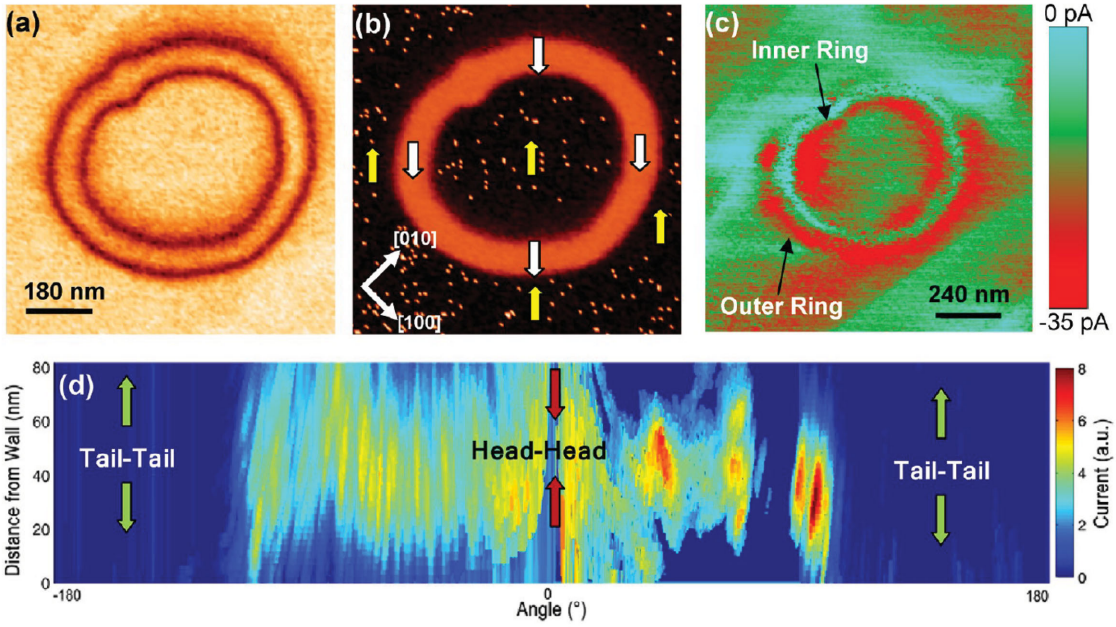

Figure 5. Topological control of conductive states due to tail–tail and head–head charges at the domain wall. a) Vertical PFM amplitude and b) phase image of a ring written by +9 V bias within a single lateral domain. The polarization vectors are shown in b. A c-AFM image, taken with $V_{tip} = -2.8$ V, is shown in (c). To better visualize the conduction map, the outer ring in c was flattened to a single 2D map and plotted in (d). Adapted with permission.[68] Copyright 2012, American Chemical Society.

domain wall around the ring structure. This would then lead to charged domain walls and hence significant (3 orders of magnitude) differences in carrier accumulation at the domain wall can be expected. [66]

A parallel model put forward by Noheda et al. is based on the idea that the conductivity is controlled by oxygen vacancies.[55] Similarly, the observation of tunable electronic conductivity at domain walls in La-doped BFO was linked to oxygen vacancy concentration (**Figure 6**).[43] One advantage of thin film oxide epitaxy is that growth conditions can be easily tuned to produce varying amounts of vacancies within the ordered stripe domain patterns.[69] The conductivity at 109° walls in such BFO samples was shown to be thermally activated with activation energies of 0.24 to 0.5 eV.

Indeed intentional defect accumulation at domain walls has recently evolved as a potent method to tailor the electronic structure at walls. This is demonstrated by a variety of methods, including conventional chemical doping and strain-driven diffusion in ferroelectric and ferroeleastic oxides. The idea of walls within walls is based on the concept of topological defects that can be precisely positioned within walls;[70] this provides an unprecedented technique to engineer functionality with precise control at the nanoscale. From a broader perspective, such approaches make it possible to induce an insulator-metal transition locally within the confines of the domain wall. We already know that through careful design of the level of dopant interaction, one can tune at will the electronic structure, the state of strain and chemical effects at the domain wall. For example by A-site doping with Ca[71–73] we already know the dipolar interactions can be modified to introduce varying amounts of oxygen vacancies which alters the electronic conductivity of BFO and can even provide a transition from n-type to p-type conduction.[72] On the horizon is the so far little explored option of magnetic B-site substitution such as Cu, Co or Ni for BFO. This might prove to be a viable way

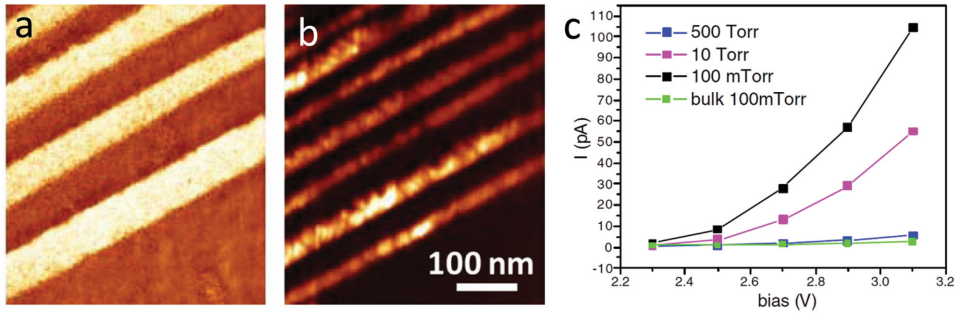

Figure 6. a) PFM image showing ordered 109° stripe domains in BFO. b) Simultaneously acquired c-AFM image of the same area showing that each 109° domain wall is electrically conductive. c) Current levels for samples with different oxygen cooling pressure and thus varying density of oxygen vacancies. Adapted with permission.[43] Copyright 2010, American Physical Society.

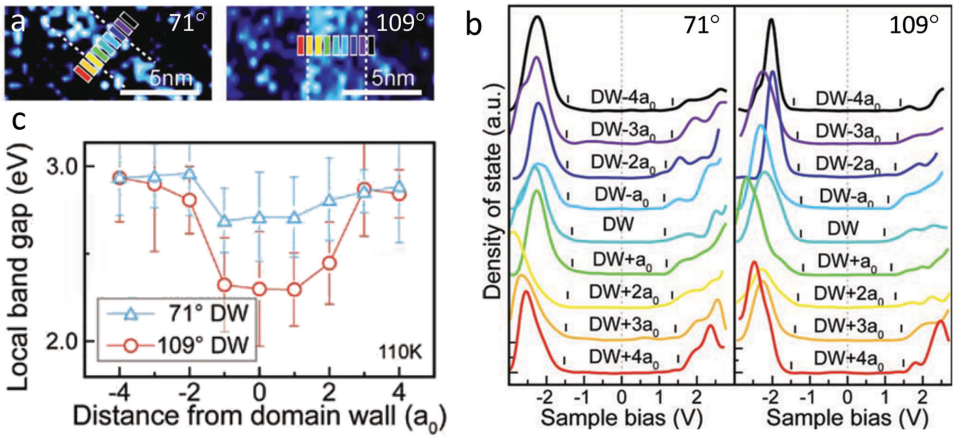

Figure 7. Layer-by-layer dI/dV measurements across 71° and 109° domain walls in BFO acquired at 110 K. Bars in (a) denote positions where the electronic spectra are probed, and (b) show the corresponding STS spectra. The band edges are indicated by black tick marks in (b). c) Extracted local band gap across the domain walls. Adapted with permission.[53]

to achieve new domain wall properties by manipulating both the spin-lattice as well as strain-lattice couplings leading the way to "magnetoelectric domain walls" by combining electronic conduction with electric and magnetic degrees of freedom.[74–76]

4. Light Interaction with Multiferroic Domain Walls

In 2010 it was shown that BFO exhibits an anomalous photovoltaic effect in thin films that arises due to a topological defect – namely, structurally driven steps of the electrostatic potential at nanometer-scale domain walls.[77–79] The mechanism for charge-separation in domain wall driven photovoltaic effect is fundamentally different for the conventional solid-state photovoltaics, where electron–hole pairs are created by light absorption in a semiconductor and separated by the electric field spanning a micrometer-thick depletion region. In the case of domain walls the relevant distance can be only a few (1–2) nm and the voltages produced are significantly higher than the bandgap. c-AFM studies performed under illumination have found that the high photovoltages to be associated with 71° and 109° domain walls in BFO.[77] Yang et al. postulate that the nanoscale steps of the electrostatic potential (created by periodic domain walls) drive the photovoltaic effect in BFO. Recent results from Alexe et al. give an alternate point of view where they argue the effect stems from a bulk effect.[80] Clearly this is an area where further studies are needed. For example, recently Rappe et al. proposed[81] similar domain-wall-based photovoltaic effects in organic perovskites. The key advantage of engineering a ferroic material where a domain-wall driven photovoltaic effect is dominant is the ability to modulate the strength of the effect via the application of an electric field. Clearly, electric-field control of the photovoltaic effect in ferroelectrics is an area of rising interest and one that we expect to enrapture the community.

The key challenge in this field is the overall conductivity of the ferroelectric material. Ironically, while leakage undermines the use of a ferroelectric significantly in ferroelectric memory and electromechanical applications, low band-gap ferroelectrics have found to be very successful as photo-ferroelectrics with some of the highest conversion efficiencies reported.[82,83] What the community needs to engineer is effective methods that would increase the carrier mobility and/or induce a spatially periodic potential without compromising the innate ferroelectric properties. For example, creating localised materials with a lower gap than BFO are possible routes to achieve larger current densities under white light illumination, and more generally, they would demonstrate what the source of periodic potential and the PV current flow can be in different materials. However since the matrix is still with relatively high band gap it would mean the leakage and related reliability issues would not severely affect ferroelectric performance. An alternate approach is low band-gap ferroelectric semiconductors with asymmetric electron and hole mobilities for dedicated use as photovoltaic materials. In addition, photoelectrochemic effects at domain walls are a possible further interesting route, e.g. for applications in water splitting.[84,85]

5. Local Density of States at Multiferroic Domain Walls

STM and Scanning Tunneling Spectroscopy (STS) measurements in cross-sectional samples have been used to directly investigate the nature of the local electronic conductivity at ferroelectric domain walls in multiferroic BFO.[53] Samples with engineered stripe domain array were used in order to simplify the location of a single wall in the STM setup for local spectroscopy. It was found that in-situ cleaved samples with ordered stripe arrays show decreases of the bandgap at the domain boundaries (**Figure 7**). In addition, a shift towards the Fermi level in the band edges of 109° and 71° domain walls have been observed. The demonstrated approach in this work serves as a model technique to investigate and understand electronic structure at complex oxide interfaces, although it is obviously limited to materials with relatively small bandgaps.

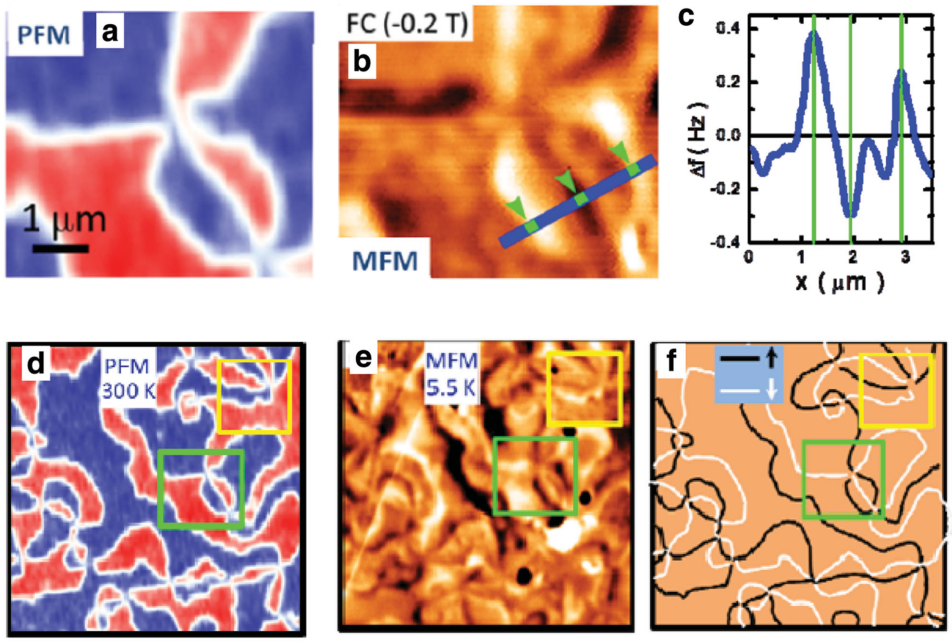

Figure 8. MFM and PFM of ErMnO3 single crystal. a) PFM image showing the up (red) and down (blue) domains, with a central junction (vortex core), taken at room temperature. MFM of the same location, taken at 5.5K, is shown in (b). Profile along the blue line is shown in (c), and indicates clear contrast at domain walls, along with inversion. d) PFM map at 300K, e) MFM map at 5.5K of a larger area (18 μm × 18 μm) and f) schematic showing the contrast in the MFM image at the domain walls. Reproduced with permission.[144] Copyright 2012, American Chemical Society.

6. Magnetic Properties of Multiferroic Domain Walls

An important aspect of the multiferroic domain walls in BFO concerns their true state of magnetism. Temperature-dependent transport measurements have been performed and are a possible route to follow to understand the actual spin structure and whether it exhibits a glasslike or ordered ferromagnetic state.[86–88] Of additional interest is the effect of extra carriers introduced into the system, e.g., by doping or electric gating, on magnetism. This includes doping with magnetic ions like Co or Ni. Is there a way to change the magnetic interaction from superexchange to double exchange in BFO, perhaps exclusively at the walls? The strength of the coupling between the ferroelectric and antiferromagnetic walls in BFO is an issue that still needs to be resolved from both a theoretical and an experimental perspective. The role of the dimensionality on electrical and magnetoelectrical transport needs to be elucidated and put into perspective with regard to known systems, such as manganites.[89,90] Recently, a notable magnetoelectric effect has been observed due to the coexistence of different spiral-spin domains and the motion of the multiferroic domain walls in $DyMnO_3$.[91,92] The interaction between ferroelectric and antiferromagnetic domain walls has been studied in model multiferroics such as $YMnO_3$[93] and BFO.[94] Magnetic force microscopy of hexagonal manganites reveal finite magnetic moments at the walls in an otherwise antiferromagnetic matrix.[95] In both cases it has been shown that the antiferromagnetic domain walls are significantly wider (by ~1–2 orders of magnitude) compared to the ferroelectric walls. This is also in agreement with the phenomenological predictions of Daraktchiev et al. for order-parameter coupling-mediated wall broadening.[96]

In addition to bismuth ferrite, the properties of multiferroic domain walls have also been studied in the hexagonal rare-earth manganites, such as $YMnO_3$[97] and $ErMnO_3$.[98,99] In these systems, the ferroelectricity is improper, arising from a structural distortion called trimerization, and results in the formation of charged domain walls along with vortex networks consisting of junctions between antiphase domain boundaries.[100–102] A significant body of literature on this topic, on both the theoretical[97,103–108] and experimental[58,107,109–111] aspects, has been building on this topic for the past decade, due to advances in both first principles theory as well as in experimental setups that are capable of exploring the magnetic interactions in single crystal samples at cryogenic temperatures (T_N ~ <120K for most rare-earth hexagonal manganites).

In order to study the cross-coupling between the ferroic orders, magnetic force microscopy (MFM) combined with piezoresponse force microscopy can offer tantalizing glimpses to the multiferroic nature of the topological defects in these systems. Wu et al.[112] have explored the vortex antivortex network of topological defects that arise on the surface of $ErMnO_3$ through this method, with the results shown in **Figure 8**. The PFM image clearly shows the interlocked structural phases which meet at a domain junction (a vortex core). Previous studies have shown that the domain walls in $YMnO_3$ can be more insulating than the bulk domains,[57] and studies of domain walls in $HoMnO_3$ suggest the presence of an out of plane polarization at the domain walls.[113] MFM, which is sensitive to the local magnetic moment, undertaken at the same region as the PFM image at 5.5K (Figure 8(b)), shows clear contrast and inversions across the different domain walls, which were suggested to be due to uncompensated Er^{3+} spins across the walls in this case.

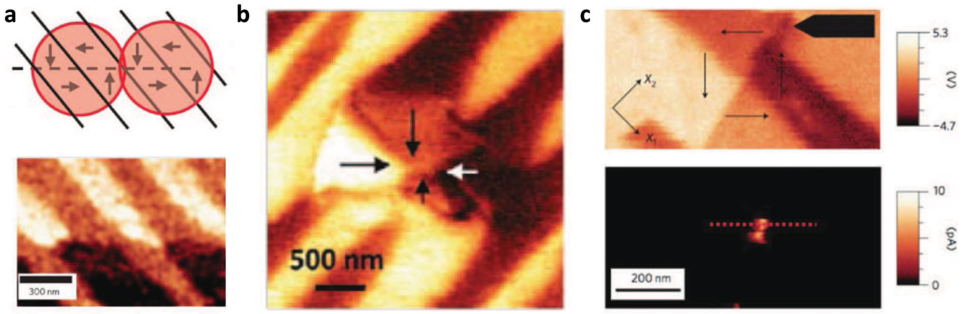

Figure 9. Vortex-like states can be created by direct writing using a SPM tip to create a) 'vortex quadrupole' chains,[145] b) 'center' domain patterns,[119] and c) enhanced conductivity has been observed at the core of flux closure domain patterns[120] in BFO. Adapted with permission from refs. [119,120] and [146]. Copyright 2009, 2011, Nature Publishing Group and 2011, American Chemical Society, respectively.

Interestingly, the magnetism appears to be correlated, at least across micron length scales (Figure 8(c,d)), suggesting a new route towards harnessing magnetoelectric coupling for nanoelectronic applications. Very recently, Geng et al.[114] have shown the potential to map the magnetoelectric coupling with nanoscale resolution in these systems directly, via detection of the electric field-induced magnetization in a technique they term magnetoelectric force microscopy, and found evidence for lattice-mediated magnetoelectric coupling in $ErMnO_3$. The application of these techniques to other ferroic systems (e..g, nanodots) promises to shed new light on magnetoelectric coupling at topological defects, and is especially pertinent as the structures first predicted to exhibit novel forms of ferroic order by Naumov et al.[115] are now beginning to be synthesized.[116,117]

7. Multiferroic Vortex Structures

The investigation of topological structures beyond the previously described domain walls are also a new exciting area of research. Ferroelectric nanowires have been shown to contain e.g. switchable quadrupoles (**Figure 9**a) which makes them interesting for nano-device applications.[118] Such vortex structures are currently a very active area of research. From thermodynamic considerations, vortex structures are only expected in limited cases in nanoscale systems when charge screening is poor, as the depolarization field dominates the elastic energy cost of the disclination center formed from adopting a vortex pattern, rendering the vortex stable. However, in thin films, such (meta-stable) states can still be formed via direct writing of the four quadrants with an SPM tip. The use of scanning probe microscopy to 'write' specific domain topologies was further developed by Vasudevan et al.[119] using pulsed fields from the scanning probe tip specifically at BFO domain walls (Figure 9b). Indeed, the vortex cores in BFO have been demonstrated to be dynamic conductors controlled by the coupled response of polarization and electron–mobile-vacancy subsystems with external bias (Figure 9c), and are apparently substantially more conductive than domain walls.[120] Indeed, a range of interesting dipole patterns surrounding domain wall junctions was investigated with close views on intersections or vertices at a very fine scale using AFM tips. The ability to create new topological structures, rather than just observing their properties holds promise for future investigations. Moreover, the elastic properties of such cores has yet to be determined, along with whether such states can be moved by fields as whole entities, similar to domain walls, which could be critical for future device applications as movable 2D nanowires.

Nelson et al., in their work on cross-sections of BFO films, show that the details of the domain patterns that form close to interfaces are dependent on whether or not the interfaces concerned sustain charge compensation.[121] At metallic interfaces stripe domains formed while at insulating interfaces small triangular domains were observed. This study shows that the local dipole orientations at non-compensating junctions reduce depolarizing fields and it also exemplifies the involvement of regions of continuous polar rotations (which, until recently, had not been observed directly in ferroelectrics).

More recently, there has been a push to investigate and actively control the properties of charged domain walls in standard ferroelectrics, given that they can act as mobile 'doping centers'. To date, two main methods have been utilized. For $BaTiO_3$ crystals, Sluka et al.[122] showed that through a 'frustrated poling' procedure during cooling of the crystal, it becomes possible to form head-head and tail-tail domain patterns. Subsequent investigations of these charged walls revealed a very large (10^9) increase in the conductivity of the walls when compared to the bulk domains, which was reasoned to originate from carriers generated through band-bending at the interfaces. More recently, the group of Nava Setter showed that in $(Bi_{0.9}La_{0.1})FeO_3$ (BLFO), by growing the films on orthrohombic substrates to restrict the possible polarization variants and subsequently using the local field of a scanning probe tip, rows of charged domain walls with increased conductivity could be generated, thus utilizing polarization charge as a quasi-dopant in the system.[123] These walls showed metallic-like conductivity, as opposed to thermally activated transport at nominally uncharged walls. The situation is similar to the discovery of tunable conductivity in ferroelectric nanodomains by Maksymovych et al.[124] Such studies show the promise of using charged walls to initiate local metal-insulator transitions at nanoscopic regimes in a reconfigurable manner.

Of course, proper understanding requires determining the actual atomic scale structure at the topological defect of interest, so the structure-property relation can be elucidated. For the

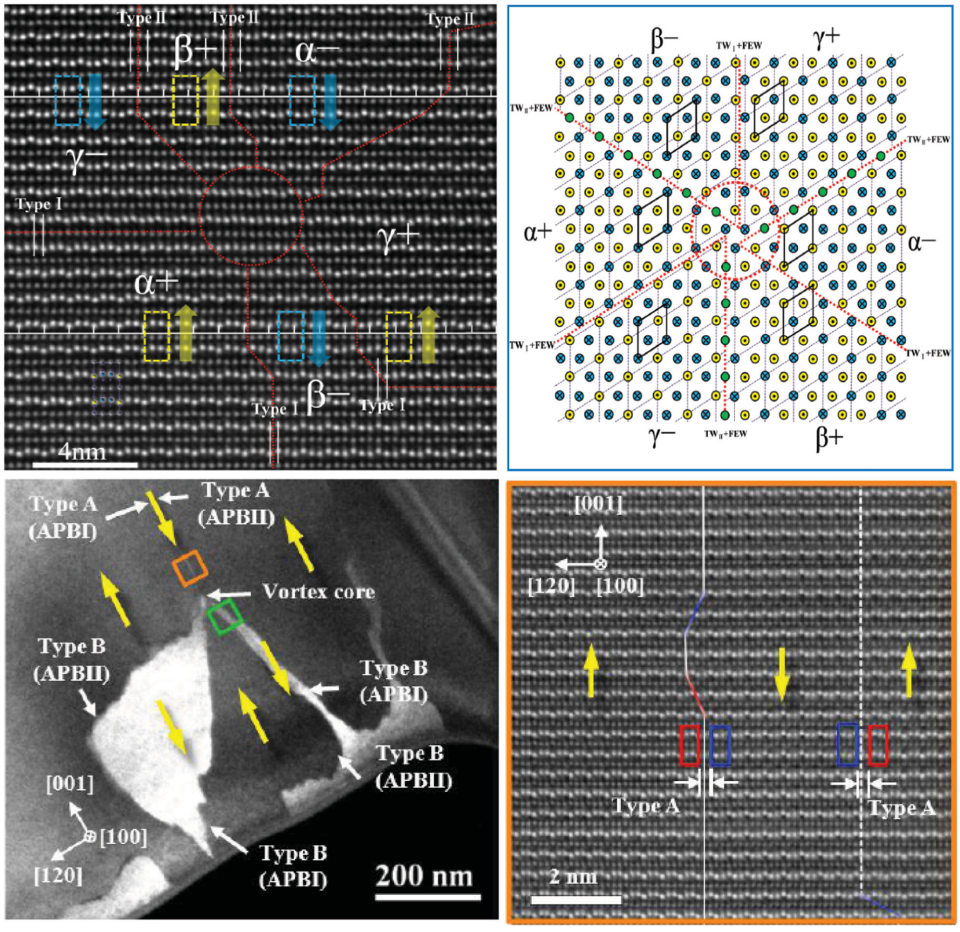

Figure 10. Atomically resolved images of multiferroic vortex cores in hexagonal manganites. (a) HAADF image of antivortex domains in $YMnO_3$, and (b) Schematic of the antivortex structure. Taken from. (c) Dark field image of a vortex in $ErMnO_3$, and (d) ADF STEM image from the orange square in (c). Yellow arrows indicate polarization directions. Reproduced with permission.[125]

hexagonal manganites, this is the vortex or antivortex core, as well as the phase boundary or domain walls themselves. Advances in electron microscopy have facilitated the imaging of both vortex and antivortex topological defects with atomic resolution (**Figure 10**).[100,125] These studies have shown that the antivortex core consists of about four unit cells in $YMnO_3$, and the atomic structure confirms the presence of changed walls around the core. The ferroelectric switching at the defect has also been investigated using in-situ STEM methods, with results showing that while the vortex core remains immobile, during switching each of the three pairs of domains switch partners in what is termed by the authors as "topologically guided partner changing". These studies confirm the nature of the defect in terms of structure, and further in-situ electron microscopy studies promise much greater structure-property relations, e.g. in determining magnetoelectric coupling at isolated defects.

8. Multiferroic Skyrmion Systems

Given the fact that strain and magnetization are only very weakly coupled in ferromagnetic systems (as compared to most ferroelectric/ferroelastic systems), it is unsurprising that there are a plethora of interesting topological defects present in these systems. For example, more complicated spin order in magnetic materials is often stabilized in noncentrosymmetric crystal lattices due to the existence of the Dzyaloshinsky-Moriya (DM) interaction. Recently, the formation of novel whirl-like spin textures called skyrmions on length scales of 10 to 100 nm has been observed in chiral magnets.[126,127] The term skyrmion was originally introduced by Skyrme as a model in nuclear physics to describe a localized, particle-like, configuration in field theory.[128] The typical two-dimensional spin texture corresponding to a single skyrmion is shown in **Figure 11**a. This spin texture is characterized by a so-called winding number and topologically stable. After several theoretical proposals the experimental observation of magnetic skyrmions was first reported for metallic alloys such as MnSi, FeGe, and $Fe_xCo_{1-x}Si$ by neutron scattering, by Lorentz transmission electron microscopy (LTEM), and magnetic force microscopy (MFM).[15]

Interestingly, skyrmions have recently been observed in an insulating multiferroic material, namely Cu_2OSeO_3 by Seki et al.[129] The application of magnetic field H leads to formation of a hexagonal lattice of skyrmions within a plane normal to H in this material only in a narrow H–T region just below

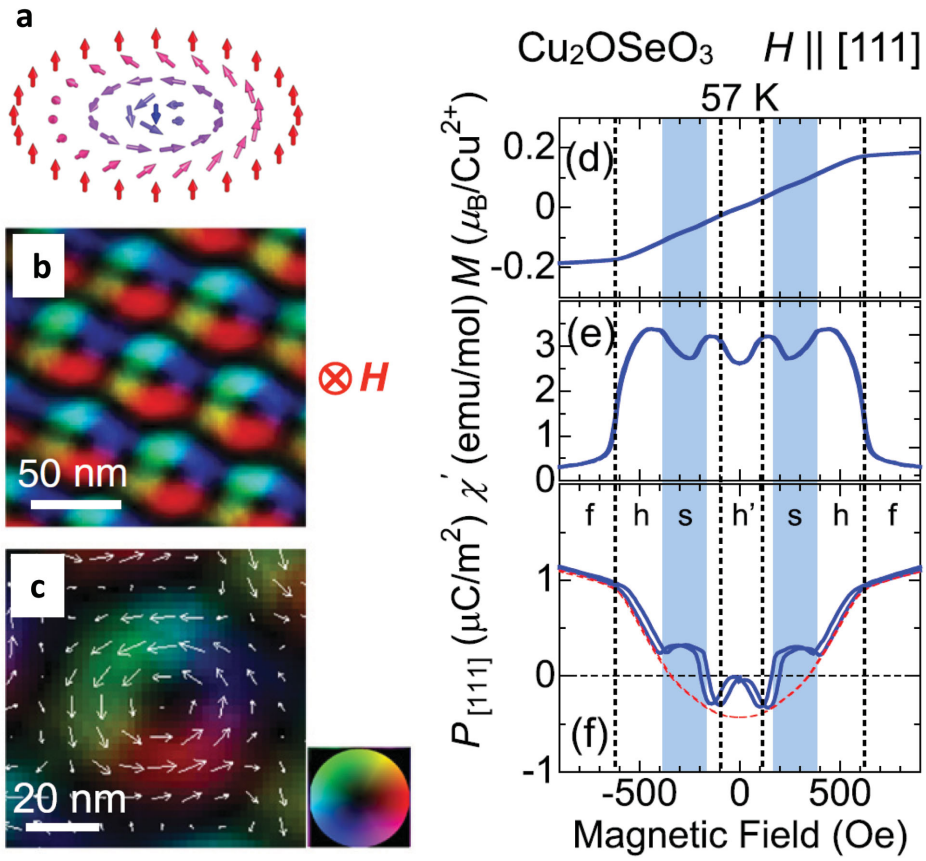

Figure 11. Skyrmions in multiferroic Cu_2OSeO_3 after Seki et al.[129] (a) schematic vector representation of single skyrmion, (b) and (c) lateral magnetization distribution map for the (110) plane of a thin-film (~100 nm thick) sample of Cu_2OSeO_3 by Lorentz-TEM at 5K, H ~ 800 Oe (white arrows represent the magnetization, color wheel shows the direction (hue) and magnitude (brightness) of the lateral magnetization. (d) to(f) magnetic field (H ∥ [111]) dependence of magnetizationM, ac magnetic susceptibility (χ'), and [111] component of electric polarization (P[111]) at 57 K. Red dashed line is the numerical fit for the single-domain helimagnetic state. Lett. f, h, h', and s denote ferrimagnetic, helimagnetic (single q domain), helimagnetic (multiple q domains), and skyrmion crystal states, respectively. Adapted with permission.[129] Copyright 2012, American Association for Advancement of Science.

Tc. In thin films it is stabilized over a wider H–T range. Similar magnetic phase diagrams have also been reported for the metallic alloys that show skyrmions. The skyrmion spin texture in Cu_2OSeO_3 can lead to spin-driven electric polarization, indicating magnetoelectric coupling in this material.

Figure 11d–f shows the magnetic field dependence of magnetization, ac magnetic susceptibility, and electric polarization along the [111] for bulk Cu_2OSeO_3. When the hexagonal skyrmion lattice is formed in the material with a small applied magnetic field, the system can become polar along the magnetic field direction. The local magnetoelectric coupling in this case leads to skyrmions carrying an electric dipole or quadrupole.[130] For single skyrmions existing in a ferromagnetic background close to the ferromagnetic state of the material, such a magnetoelectric skyrmion can be moved and manipulated by the spatial gradient of an electric field. Thus, magnetoelectric skyrmions may contribute to the design of novel low-dissipation spintronic devices.

Several studies to manipulate skyrmions in insulators by electric field have already been presented.[131] Small angle neutron scattering experiments show that the application of electric fields can cause a slight rotation of the skyrmion crystal.[131] The hexagonal skyrmion crystal also shows unique magnetic resonance properties under an oscillating magnetic field in the GHz range.[132,133] Local magnetoelectric coupling allows for the activation of these excitations also by alternating electric fields (i.e. electromagnon excitation).[134,135] For a full review that focuses on spin-driven ferroelectricity we refer the reader to recent review by Tokura et al[138]

9. Outlook

Topological structures in multiferroics, namely domain walls, vortices and skyrmions form an exciting and growing field of interest in functional materials. The field has seen rapid developments; nevertheless there are many remaining questions and new areas to be explored. Firstly, what are the theoretical principles governing topological defect stuctures? Spaldin and co-workers have recently looked into the Landau theory of topological defects, particularly in hexagonal manganites.[106] Similarly, using a hybrid approach, L. Q. Chen et al have investigated the hierarchies of the wall energies in BFO and link the energies in particular domain walls to the twist in the oxygen

octahedral rotations.[133] From an experimentalists' perspective, a predictive theory, which identifies the boundary conditions under which topological structures can be created at will would be immensely powerful.

The investigation of dynamic conductivity at domain walls is an exciting aspect,[134] which is linked to factors such as possible electric-field induced distortion of the polarization structure at the domain wall, the dependence of conductivity on the degree of distortion and how weak-pinning scenarios affect the domain wall. The domain wall is very likely not a rigid electronic conductor but rather one that posseses a quasi-continuous spectrum of voltage-tunable electronic states. This would give the domain wall memristor properties in contrast to domains, which were shown to exhibit concrete conductance levels.[31] The intrinsic dynamics of domain walls and other topological defects are expected not only to influence future theoretical and experimental interpretations of the electronic phenomena, but also pose a possibility to find unique properties of multiferroic domain walls, e.g. magnetization and magnetoresistance within an insulating antiferromagnetic matrix, influenced by order parameter coupling and localized secondary order parameters.[10,139] The observation of superconductivity in ferroelastic walls of WO_3 is an indication of various exciting and unexplored areas of domain boundary physics.[135] The tantalizing opportunity of being able to controllably induce electronic phase transitions within the wall due to specific physical interactions would give rise to "designer domain wall electronics". Indeed we stand at a threshold of a new era where domain-wall based phenomena will underpin a plethora of applications[9] such as a local strain sensor incorporated on an AFM probe, reconfigurable nanocircuits or a multilevel resistance-state device that is written by an electrical current,[136] nonvolatile memories, piezoelectric actuators, ultrasound transducers, surface acoustic wave devices and optical applications and nanoscale magneto-electric applications.[93,96,137,138]

Although initially the excitement around topological defects in ferroic systems stemmed from the prediction of ferrotoroidic phase transitions in ferroelectric nanodots, which have thus far not actually been seen, the field has rapidly spread to determining the local functional properties of other topological defects in both mesoscopic and macroscopic systems, both intrinsic and engineered. The controlled generation and manipulation of topological defects by strain and elecric fields promises to be a continued playground for exploring novel physics at singularities and interfaces, and will continue to do so with advances in both scanning probe and electron microscopies allow functional properties and polarization vectors to be mapped at the single unit cell level.

Acknowledgements

JS and VN acknowledge support by the Australian Research Council through ARC Discovery Projects. JS also acknowledges an ARC Future Fellowship. This research was in part sponsored by the Division of Materials Sciences and Engineering, BES, DOE (RKV). We acknowledge fruitful discussions with all our colleagues, and in particular wish to extend a special thanks to all participants of the "International Workshop on Topological Structures in Ferroic Materials" held in Sydney in May 2015. He also acknowledges the help of Mr. Dongyi Zhou in maintaining the reference list for this article.

Received: September 1, 2015
Revised: October 12, 2015
Published online: December 15, 2015

[1] T. W. Kibble, *J. Phys. A: Math. Gen.* **1976**, *9*, 1387.
[2] I. Chuang, R. Durrer, N. Turok, B. Yurke, *Science* **1991**, *251*, 1336.
[3] A. Maniv, E. Polturak, G. Koren, *Phys. Rev. Lett.* **2003**, *91*, 197001.
[4] C. Bäuerle, Y. M. Bunkov, S. Fisher, H. Godfrin, G. Pickett, *Nature* **1996**, *382*, 332.
[5] N. D. Mermin, *Rev. Mod. Phys.* **1979**, *51*, 591.
[6] J. F. Scott, *Science* **2007**, *315*, 954.
[7] S. S. Parkin, Spin Dependent Transport in Magnetic Nanostructures (Eds: S. Maekawa, Teruya Shinjo), *Advances in Condensed Matter Science*, Taylor & Francis, London **2002**, 292.
[8] J. Seidel, *Nat. Nanotechnol.* **2015**, *10*, 109.
[9] J. Seidel, *J. Phys. Chem. Lett.* **2012**, *3*, 2905.
[10] S. Farokhipoor, C. Magen, S. Venkatesan, J. Iniguez, C. J. M. Daumont, D. Rubi, E. Snoeck, M. Mostovoy, C. de Graaf, A. Muller, M. Doblinger, C. Scheu, B. Noheda, *Nature* **2014**, *515*, 379.
[11] K. E. Kim, B. K. Jang, Y. Heo, J. H. Lee, M. Jeong, J. Y. Lee, J. Seidel, C. H. Yang, *NPG Asia Mater.* **2014**, *6*, e81.
[12] Y. Heo, B. K. Jang, S. J. Kim, C. H. Yang, J. Seidel, *Adv. Mater.* **2014**, *26*, 7568.
[13] J. H. Lee, K. Chu, A. A. Unal, S. Valencia, F. Kronast, S. Kowarik, J. Seidel, C. H. Yang, *Phys. Rev. B* **2014**, *89*, 140101(R).
[14] J. X. Zhang, B. Xiang, Q. He, J. Seidel, R. J. Zeches, P. Yu, S. Y. Yang, C. H. Wang, Y. H. Chu, L. W. Martin, A. M. Minor, R. Ramesh, *Nat. Nanotechnol.* **2011**, *6*, 97.
[15] P. Milde, D. Kohler, J. Seidel, L. M. Eng, A. Bauer, A. Chacon, J. Kindervater, S. Muhlbauer, C. Pfleiderer, S. Buhrandt, C. Schutte, A. Rosch, *Science* **2013**, *340*, 1076.
[16] I. I. Naumov, L. Bellaiche, H. Fu, *Nature* **2004**, *432*, 737.
[17] S. Griffin, M. Lilienblum, K. Delaney, Y. Kumagai, M. Fiebig, N. Spaldin, *Phys. Rev. X* **2012**, *2*, 041022.
[18] P. Zubko, S. Gariglio, M. Gabay, P. Ghosez, J. M. Triscone, *Annu. Rev. Condens. Matter Phys.* **2011**, *2*, 141.
[19] R. K. Vasudevan, W. D. Wu, J. R. Guest, A. P. Baddorf, A. N. Morozovska, E. A. Eliseev, N. Balke, V. Nagarajan, P. Maksymovych, S. V. Kalinin, *Adv. Funct. Mater.* **2013**, *23*, 2592.
[20] A. Pramanick, A. D. Prewitt, J. S. Forrester, J. L. Jones, *Crit. Rev. Solid State Mater. Sci.* **2012**, *37*, 243.
[21] C. T. Nelson, P. Gao, J. R. Jokisaari, C. Heikes, C. Adamo, A. Melville, S.-H. Baek, C. M. Folkman, B. Winchester, Y. Gu, *Science* **2011**, *334*, 968.
[22] C. L. Jia, M. Lentzen, K. Urban, *Science* **2003**, *299*, 870.
[23] C.-L. Jia, S.-B. Mi, K. Urban, I. Vrejoiu, M. Alexe, D. Hesse, *Nat. Mater.* **2008**, *7*, 57.
[24] A. Lubk, M. D. Rossell, J. Seidel, Y. H. Chu, R. Ramesh, M. J. Hytch, E. Snoeck, *Nano Lett.* **2013**, *13*, 1410.
[25] K. Urban, *Advances in Imaging and Electron, Physics*, Vol. *153*, Elsevier, New York **2008**.
[26] C. L. Jia, K. Urban, *Science* **2004**, *303*, 2001.
[27] P. Gao, C. T. Nelson, J. R. Jokisaari, S.-H. Baek, C. W. Bark, Y. Zhang, E. Wang, D. G. Schlom, C.-B. Eom, X. Pan, *Nat. Commun.* **2011**, *2*, 591.
[28] M. D. Rossell, R. Erni, M. P. Prange, J. C. Idrobo, W. Luo, R. J. Zeches, S. T. Pantelides, R. Ramesh, *Phys. Rev. Lett.* **2012**, *108*, 047601.

[29] C. L. Jia, V. Nagarajan, J. Q. He, L. Houben, T. Zhao, R. Ramesh, K. Urban, R. Waser, *Nat. Mater.* **2007**, *6*, 64.
[30] C. L. Jia, S. B. Mi, K. Urban, I. Vrejoiu, M. Alexe, D. Hesse, *Nat. Mater.* **2008**, *7*, 57.
[31] J. Seidel, L. W. Martin, Q. He, Q. Zhan, Y. H. Chu, A. Rother, M. E. Hawkridge, P. Maksymovych, P. Yu, M. Gajek, N. Balke, S. V. Kalinin, S. Gemming, F. Wang, G. Catalan, J. F. Scott, N. A. Spaldin, J. Orenstein, R. Ramesh, *Nat. Mater.* **2009**, *8*, 229.
[32] A. Y. Borisevich, H. J. Chang, M. Huijben, M. P. Oxley, S. Okamoto, M. K. Niranjan, J. D. Burton, E. Y. Tsymbal, Y. H. Chu, P. Yu, R. Ramesh, S. V. Kalinin, S. J. Pennycook, *Phys. Rev. Lett.* **2010**, *105*, 087204.
[33] A. Lubk, M. D. Rossell, J. Seidel, Q. He, S. Y. Yang, Y. H. Chu, R. Ramesh, M. J. Hytch, E. Snoeck, *Phys. Rev. Lett.* **2012**, *109*, 047601.
[34] J. Seidel, M. Trassin, Y. Zhang, P. Maksymovych, T. Uhlig, P. Milde, D. Kohler, A. P. Baddorf, S. V. Kalinin, L. M. Eng, X. Q. Pan, R. Ramesh, *Adv. Mater.* **2014**, *26*, 4376.
[35] L. M. Eng, *Nanotechnology* **1999**, *10*, 405.
[36] V. R. Aravind, A. N. Morozovska, S. Bhattacharyya, D. Lee, S. Jesse, I. Grinberg, Y. L. Li, S. Choudhury, P. Wu, K. Seal, A. M. Rappe, S. V. Svechnikov, E. A. Eliseev, S. R. Phillpot, L. Q. Chen, V. Gopalan, S. V. Kalinin, *Phys. Rev. B* **2010**, *82*, 024111.
[37] R. K. Vasudevan, M. B. Okatan, C. Duan, Y. Ehara, H. Funakubo, A. Kumar, S. Jesse, L. Q. Chen, S. V. Kalinin, V. Nagarajan, *Adv. Funct. Mater.* **2013**, *23*, 81.
[38] S. V. Kalinin, A. N. Morozovska, L. Q. Chen, B. J. Rodriguez, *Rep. Prog. Phys.* **2010**, *73*, 056502.
[39] A. Gruverman, B. J. Rodriguez, C. Dehoff, J. D. Waldrep, A. I. Kingon, R. J. Nemanich, J. S. Cross, *Appl. Phys. Lett.* **2005**, *87*, 082902.
[40] B. J. Rodriguez, S. Jesse, A. P. Baddorf, T. Zhao, Y. H. Chu, R. Ramesh, E. A. Eliseev, A. N. Morozovska, S. V. Kalinin, *Nanotechnology* **2007**, *18*, 405701.
[41] T. Jungk, A. Hoffmann, E. Soergel, *J. Appl. Phys.* **2007**, *102*, 084102.
[42] C. H. Yang, J. Seidel, S. Y. Kim, P. B. Rossen, P. Yu, M. Gajek, Y. H. Chu, L. W. Martin, M. B. Holcomb, Q. He, P. Maksymovych, N. Balke, S. V. Kalinin, A. P. Baddorf, S. R. Basu, M. L. Scullin, R. Ramesh, *Nat. Mater.* **2009**, *8*, 485.
[43] J. Seidel, P. Maksymovych, Y. Batra, A. Katan, S. Y. Yang, Q. He, A. P. Baddorf, S. V. Kalinin, C. H. Yang, J. C. Yang, Y. H. Chu, E. K. H. Salje, H. Wormeester, M. Salmeron, R. Ramesh, *Phys. Rev. Lett.* **2010**, *105*, 197603.
[44] W. Fan, J. Cao, J. Seidel, Y. Gu, J. W. Yim, C. Barrett, K. M. Yu, J. Ji, R. Ramesh, L. Q. Chen, J. Wu, *Phys. Rev. B* **2011**, *83*, 235102.
[45] B. J. Rodriguez, Y. H. Chu, R. Ramesh, S. V. Kalinin, *Appl. Phys. Lett.* **2008**, *93*, 142901.
[46] J. Seidel, W. Luo, S. J. Suresha, P. K. Nguyen, A. S. Lee, S. Y. Kim, C. H. Yang, S. J. Pennycook, S. T. Pantelides, J. F. Scott, R. Ramesh, *Nat. Comm.* **2012**, *3*, 799.
[47] N. Balke, S. Jesse, A. N. Morozovska, E. Eliseev, D. W. Chung, Y. Kim, L. Adamczyk, R. E. Garcia, N. Dudney, S. V. Kalinin, *Nat. Nanotechnol.* **2010**, *5*, 749.
[48] A. Kumar, F. Ciucci, A. N. Morozovska, S. V. Kalinin, S. Jesse, *Nat. Chem.* **2011**, *3*, 707.
[49] Y. M. Kim, J. He, M. D. Biegalski, H. Ambaye, V. Lauter, H. M. Christen, S. T. Pantelides, S. J. Pennycook, S. V. Kalinin, A. Y. Borisevich, *Nat. Mater.* **2012**, *11*, 888.
[50] A. Wiessner, J. Kirschner, G. Schafer, T. Berghaus, *Rev. Sci. Instrum.* **1997**, *68*, 3790.
[51] B. Yang, N. J. Park, B. I. Seo, Y. H. Oh, S. J. Kim, S. K. Hong, S. S. Lee, Y. J. Park, *Appl. Phys. Lett.* **2005**, *87*, 062902.
[52] R. E. Garcia, B. D. Huey, J. E. Blendell, *J. Appl. Phys.* **2006**, *100*, 064105.
[53] Y. P. Chiu, Y. T. Chen, B. C. Huang, M. C. Shih, J. C. Yang, Q. He, C. W. Liang, J. Seidel, Y. C. Chen, R. Ramesh, Y. H. Chu, *Adv. Mater.* **2011**, *23*, 1530.
[54] B. M. Vul, G. M. Guro, I. I. Ivanchik, *Ferroelectrics* **1973**, *6*, 29.
[55] S. Farokhipoor, B. Noheda, *Phys. Rev. Lett.* **2011**, *107*, 127601.
[56] J. Seidel, G. Singh-Bhalla, Q. He, S. Y. Yang, Y. H. Chu, R. Ramesh, *Phase Transitions* **2013**, *86*, 53.
[57] T. Choi, Y. Horibe, H. T. Yi, Y. J. Choi, W. D. Wu, S. W. Cheong, *Nat. Mater.* **2010**, *9*, 253.
[58] D. Meier, J. Seidel, A. Cano, K. Delaney, Y. Kumagai, M. Mostovoy, N. A. Spaldin, R. Ramesh, M. Fiebig, *Nat. Mater.* **2012**, *11*, 284.
[59] A. Lubk, S. Gemming, N. A. Spaldin, *Phys. Rev. B* **2009**, *80*, 104110.
[60] O. Diéguez, P. Aguado-Puente, J. Junquera, J. Íñiguez, *Phys. Rev. B* **2013**, *87*, 024102.
[61] Z. Gareeva, O. Diéguez, J. Íñiguez, A. K. Zvezdin, *Phys. Rev. B* **2015**, *91*, 060404.
[62] M. D. Rossell, R. Erni, M. P. Prange, J. C. Idrobo, W. Luo, R. J. Zeches, S. T. Pantelides, R. Ramesh, *Phys. Rev. Lett.* **2012**, *108*, 047601.
[63] A. Borisevich, O. S. Ovchinnikov, H. J. Chang, M. P. Oxley, P. Yu, J. Seidel, E. A. Eliseev, A. N. Morozovska, R. Ramesh, S. J. Pennycook, S. V. Kalinin, *ACS Nano* **2010**, *4*, 6071.
[64] W. Ren, Y. Yang, O. Dieguez, J. Iniguez, N. Choudhury, L. Bellaiche, *Phys. Rev. Lett.* **2013**, *110*, 187601.
[65] E. Eliseev, A. Morozovska, G. Svechnikov, V. Gopalan, V. Y. Shur, *Phys. Rev. B* **2011**, *83*, 235313.
[66] E. A. Eliseev, A. N. Morozovska, Y. Gu, A. Y. Borisevich, L.-Q. Chen, V. Gopalan, S. V. Kalinin, *Phys. Rev. B* **2012**, *86*, 085416.
[67] E. A. Eliseev, A. N. Morozovska, G. S. Svechnikov, P. Maksymovych, S. V. Kalinin, *Phys. Rev. B* **2012**, *85*, 045312.
[68] A. N. Morozovska, R. K. Vasudevan, P. Maksymovych, S. V. Kalinin, E. A. Eliseev, *Phys. Rev. B* **2012**, *86*, 085315.
[69] M. L. Scullin, J. Ravichandran, C. Yu, M. Huijben, J. Seidel, A. Majumdar, R. Ramesh, *Acta Mater.* **2010**, *58*, 457.
[70] T. Zykova-Timan, E. K. H. Salje, *Appl. Phys. Lett.* **2014**, *104*, 082907.
[71] J. Zhou, M. Trassin, Q. He, N. Tamura, M. Kunz, C. Cheng, J. X. Zhang, W. I. Liang, J. Seidel, C. L. Hsin, J. Q. Wu, *J. Appl. Phys.* **2012**, *112*, 064102.
[72] C. H. Yang, D. Kan, I. Takeuchi, V. Nagarajan, J. Seidel, *Phys. Chem. Chem. Phys.* **2012**, *14*, 15953.
[73] A. Ikeda-Ohno, J. S. Lim, T. Ohkochi, C. H. Yang, J. Seidel, *Phys. Chem. Chem. Phys.* **2014**, *16*, 17412.
[74] K. T. Ko, M. H. Jung, Q. He, J. H. Lee, C. S. Woo, K. Chu, J. Seidel, B. G. Jeon, Y. S. Oh, K. H. Kim, W. I. Liang, H. J. Chen, Y. H. Chu, Y. H. Jeong, R. Ramesh, J. H. Park, C. H. Yang, *Nat. Commun.* **2011**, *2*, 567.
[75] M. O. Ramirez, A. Kumar, S. A. Denev, Y. H. Chu, J. Seidel, L. W. Martin, S. Y. Yang, R. C. Rai, X. S. Xue, J. F. Ihlefeld, N. J. Podraza, E. Saiz, S. Lee, J. Klug, S. W. Cheong, M. J. Bedzyk, O. Auciello, D. G. Schlom, J. Orenstein, R. Ramesh, J. L. Musfeldt, A. P. Litvinchuk, V. Gopalan, *Appl. Phys. Lett.* **2009**, *94*, 161905.
[76] M. O. Ramirez, M. Krishnamurthi, S. Denev, A. Kumar, S. Y. Yang, Y. H. Chu, E. Saiz, J. Seidel, A. P. Pyatakov, A. Bush, D. Viehland, J. Orenstein, R. Ramesh, V. Gopalan, *Appl. Phys. Lett.* **2008**, *92*, 022511.
[77] S. Y. Yang, J. Seidel, S. J. Byrnes, P. Shafer, C. H. Yang, M. D. Rossell, P. Yu, Y. H. Chu, J. F. Scott, J. W. Ager, L. W. Martin, R. Ramesh, *Nat. Nanotech.* **2010**, *5*, 143.
[78] J. Seidel, D. Y. Fu, S. Y. Yang, E. Alarcon-Llado, J. Q. Wu, R. Ramesh, J. W. Ager, *Phys. Rev. Lett.* **2011**, *107*, 126805.
[79] J. Seidel, S. Y. Yang, E. Alarcon-Llado, J. W. Ager, R. Ramesh, *Ferroelectrics* **2012**, *433*, 123.

[80] A. Bhatnagar, A. R. Chaudhuri, Y. H. Kim, D. Hesse, M. Alexe, *Nat. Commun.* **2013**, *4*, 2835.
[81] S. Liu, F. Zheng, N. Z. Koocher, H. Takenaka, F. G. Wang, A. M. Rappe, *J. Phys. Chem. Lett.* **2015**, *6*, 693.
[82] I. Grinberg, D. V. West, M. Torres, G. Y. Gou, D. M. Stein, L. Y. Wu, G. N. Chen, E. M. Gallo, A. R. Akbashev, P. K. Davies, J. E. Spanier, A. M. Rappe, *Nature* **2013**, *503*, 509.
[83] R. Nechache, C. Harnagea, S. Li, L. Cardenas, W. Huang, J. Chakrabartty, F. Rosei, *Nat. Photonics* **2015**, *9*, 61.
[84] A. Kudo, Y. Miseki, *Chem. Soc. Rev.* **2009**, *38*, 253.
[85] J. Seidel, L. M. Eng, *Curr. Appl. Phys.* **2014**, *14*, 1083.
[86] Q. He, C. H. Yeh, J. C. Yang, G. Singh-Bhalla, C. W. Liang, P. W. Chiu, G. Catalan, L. W. Martin, Y. H. Chu, J. F. Scott, R. Ramesh, *Phys. Rev. Lett.* **2012**, *108*, 067203.
[87] J. C. Yang, C. H. Yeh, Y. T. Chen, S. C. Liao, R. Huang, H. J. Liu, C. C. Hung, S. H. Chen, S. L. Wu, C. H. Lai, Y. P. Chiu, P. W. Chiu, Y. H. Chu, *Nanoscale* **2014**, *6*, 10524.
[88] J. H. Lee, I. Fina, X. Marti, Y. H. Kim, D. Hesse, M. Alexe, *Adv. Mater.* **2014**, *26*, 7078.
[89] E. Dagotto, *Nanoscale phase separation and colossal magnetoresistance: the physics of manganites and related compounds*, Vol. *136*, Springer Science & Business Media, Heidelberg, Germany **2013**
[90] J. Salafranca, R. Yu, E. Dagotto, *Phys. Rev. B* **2010**, *81*, 245122.
[91] F. Kagawa, M. Mochizuki, Y. Onose, H. Murakawa, Y. Kaneko, N. Furukawa, Y. Tokura, *Phys. Rev. Lett.* **2009**, *102*, 057604.
[92] F. Kagawa, Y. Onose, Y. Kaneko, Y. Tokura, *Phys. Rev. B* **2011**, *83*, 054413.
[93] A. V. Goltsev, R. V. Pisarev, T. Lottermoser, M. Fiebig, *Phys. Rev. Lett.* **2003**, *90*, 177204.
[94] Z. V. Gareeva, A. K. Zvezdin, *Phys. Stat. Solidi*. **2009**, *3*, 79.
[95] Y. Geng, N. Lee, Y. Choi, S.-W. Cheong, W. Wu, *Nano Lett.* **2012**, *12*, 6055.
[96] M. Daraktchiev, G. Catalan, J. F. Scott, *Phys. Rev. B* **2010**, *81*, 224118.
[97] B. B. Van Aken, T. T. M. Palstra, A. Filippetti, N. A. Spaldin, *Nat. Mater.* **2004**, *3*, 164.
[98] B. B. Van Aken, A. Meetsma, T. T. M. Palstra, *Acta Crystallogr., Sect. E: Crystallogr. Commun.* **2001**, *57*, I38.
[99] D. Meier, H. Ryll, K. Kiefer, B. Klemke, J. U. Hoffmann, R. Ramesh, M. Fiebig, *Phys. Rev. B* **2012**, *86*, 184415.
[100] Q. H. Zhang, G. T. Tan, L. Gu, Y. Yao, C. Q. Jin, Y. G. Wang, X. F. Duan, R. C. Yu, *Sci. Rep.* **2013**, *3*, 2741.
[101] Y. Kumagai, N. A. Spaldin, *Nat. Commun.* **2013**, *4*, 1540.
[102] S. C. Chae, N. Lee, Y. Horibe, M. Tanimura, S. Mori, B. Gao, S. Carr, S. W. Cheong, *Phys. Rev. Lett.* **2012**, *108*, 167603.
[103] C. J. Fennie, K. M. Rabe, *Phys. Rev. B* **2005**, *72*, 100103.
[104] S. M. Griffin, M. Lilienblum, K. T. Delaney, Y. Kumagai, M. Fiebig, N. A. Spaldin, *Phys. Rev. X* **2012**, *2*, 041022.
[105] W. S. Choi, D. G. Kim, S. S. A. Seo, S. J. Moon, D. Lee, J. H. Lee, H. S. Lee, D. Y. Cho, Y. S. Lee, P. Murugavel, J. Yu, T. W. Noh, *Phys. Rev. B* **2008**, *77*, 045137.
[106] S. Artyukhin, K. T. Delaney, N. A. Spaldin, M. Mostovoy, *Nat. Mat.* **2014**, *13*, 42.
[107] D. J. Kim, T. R. Paudel, H. D. Lu, J. D. Burton, J. G. Connell, E. Y. Tsymbal, S. S. A. Seo, A. Gruverman, *Adv. Mater.* **2014**, *26*, 7660.
[108] H. Das, A. L. Wysocki, Y. N. Geng, W. D. Wu, C. J. Fennie, *Nat. Commun.* **2014**, *5*, 2998.
[109] M. G. Han, Y. M. Zhu, L. J. Wu, T. Aoki, V. Volkov, X. Y. Wang, S. C. Chae, Y. S. Oh, S. W. Cheong, *Adv. Mater.* **2013**, *25*, 2415.
[110] F. T. Huang, X. Wang, Y. S. Oh, K. Kurushima, S. Mori, Y. Horibe, S. W. Cheong, *Phys. Rev. B* **2013**, *87*, 184109.
[111] M. Lilienblum, T. Lottermoser, S. Manz, S. M. Selbach, A. Cano, M. Fiebig, *Nat. Phys.*, DOI: 10.1038/nphys3468.
[112] Y. N. Geng, N. Lee, Y. J. Choi, S. W. Cheong, W. D. Wu, *Nano Lett.* **2012**, *12*, 6055.
[113] E. B. Lochocki, S. Park, N. Lee, S. W. Cheong, W. D. Wu, *Appl. Phys. Lett.* **2011**, *99*, 232901.
[114] Y. N. Geng, H. Das, A. L. Wysocki, X. Y. Wang, S. W. Cheong, M. Mostovoy, C. J. Fennie, W. D. Wu, *Nat. Mater.* **2014**, *13*, 163.
[115] I. I. Naumov, L. Bellaiche, H. X. Fu, *Nature* **2004**, *432*, 737.
[116] M. J. Polking, M. G. Han, A. Yourdkhani, V. Petkov, C. F. Kisielowski, V. V. Volkov, Y. M. Zhu, G. Caruntu, A. P. Alivisatos, R. Ramesh, *Nat. Mater.* **2012**, *11*, 700.
[117] X. Obradors, T. Puig, M. Gibert, A. Queralto, J. Zabaleta, N. Mestres, *Chem. Soc. Rev.* **2014**, *43*, 2200.
[118] J. W. Hong, G. Catalan, D. N. Fang, E. Artacho, J. F. Scott, *Phys. Rev. B* **2010**, *81*, 172101.
[119] R. K. Vasudevan, Y. C. Chen, H. H. Tai, N. Balke, P. P. Wu, S. Bhattacharya, L. Q. Chen, Y. H. Chu, I. N. Lin, S. V. Kalinin, V. Nagarajan, *ACS Nano* **2011**, *5*, 879.
[120] N. Balke, B. Winchester, W. Ren, Y. H. Chu, A. N. Morozovska, E. A. Eliseev, M. Huijben, R. K. Vasudevan, P. Maksymovych, J. Britson, *Nat. Phys.* **2012**, *8*, 81.
[121] C. T. Nelson, B. Winchester, Y. Zhang, S. J. Kim, A. Melville, C. Adamo, C. M. Folkman, S. H. Baek, C. B. Eom, D. G. Schlom, L. Q. Chen, X. Q. Pan, *Nano Lett.* **2011**, *11*, 828.
[122] T. Sluka, A. K. Tagantsev, P. Bednyakov, N. Setter, *Nat. Commun.* **2013**, *4*, 1808.
[123] A. Crassous, T. Sluka, A. K. Tagantsev, N. Setter, *Nat. Nanotechnol.* **2015**, *10*, 614.
[124] P. Maksymovych, A. N. Morozovska, P. Yu, E. A. Eliseev, Y.-H. Chu, R. Ramesh, A. P. Baddorf, S. V. Kalinin, *Nano Lett.* **2011**, *12*, 209.
[125] M. G. Han, Y. M. Zhu, L. J. Wu, T. Aoki, V. Volkov, X. Y. Wang, S. C. Chae, Y. S. Oh, S. W. Cheong, *Adv. Mater.* **2013**, *25*, 2415.
[126] S. Muhlbauer, B. Binz, F. Jonietz, C. Pfleiderer, A. Rosch, A. Neubauer, R. Georgii, P. Boni, *Science* **2009**, *323*, 915.
[127] X. Z. Yu, Y. Onose, N. Kanazawa, J. H. Park, J. H. Han, Y. Matsui, N. Nagaosa, Y. Tokura, *Nature* **2010**, *465*, 901.
[128] T. H. R. Skyrme, *Nucl. Phys.* **1962**, *31*, 556.
[129] S. Seki, X. Z. Yu, S. Ishiwata, Y. Tokura, *Science* **2012**, *336*, 198.
[130] S. Seki, S. Ishiwata, Y. Tokura, *Phys. Rev. B* **2012**, *86*, 060603.
[131] J. S. White, I. Levatic, A. A. Omrani, N. Egetenmeyer, K. Prsa, I. Zivkovic, J. L. Gavilano, J. Kohlbrecher, M. Bartkowiak, H. Berger, H. M. Ronnow, *J. Phys. Cond. Matt.* **2012**, *24*, 432201.
[132] M. Mochizuki, *Phys. Rev. Lett.* **2012**, *108*, 017601.
[133] Y. Onose, Y. Okamura, S. Seki, S. Ishiwata, Y. Tokura, *Phys. Rev. Lett.* **2012**, *109*, 037603.
[134] M. Mochizuki, S. Seki, *Phys. Rev. B* **2013**, *87*, 134403.
[135] Y. Okamura, F. Kagawa, M. Mochizuki, M. Kubota, S. Seki, S. Ishiwata, M. Kawasaki, Y. Onose, Y. Tokura, *Nat. Commun.* **2013**, *4*, 2391.
[136] Y. Wang, C. Nelson, A. Melville, B. Winchester, S. L. Shang, Z. K. Liu, D. G. Schlom, X. Q. Pan, L. Q. Chen, *Phys. Rev. Lett.* **2013**, *110*, 267601.
[137] P. Maksymovych, J. Seidel, Y. H. Chu, P. P. Wu, A. P. Baddorf, L. Q. Chen, S. V. Kalinin, R. Ramesh, *Nano Lett.* **2011**, *11*, 1906.
[138] Y. Tokura, S. Seki, N. Nagaosa, *Rep. Prog. Phys.* **2014**, *77*, 076501.
[139] S. Farokhipoor, B. Noheda, *Phys. Rev. Lett.* **2011**, *107*, 127601.
[140] A. Aird, E. K. H. Salje, *J. Phys. Cond. Matt.* **1998**, *10*, L377.
[141] H. Bea, P. Paruch, *Nat. Mater.* **2009**, *8*, 168.
[142] V. Skumryev, V. Laukhin, I. Fina, X. Marti, F. Sanchez, M. Gospodinov, J. Fontcuberta, *Phys. Rev. Lett.* **2011**, *106*, 057206.
[143] G. Catalan, J. Seidel, R. Ramesh, J. F. Scott, *Rev. Mod. Phys.* **2012**, *84*, 119.
[144] Y. N. Geng, N. Lee, Y. J. Choi, S. W. Cheong, W. D. Wu, *Nano Lett.* **2012**, *12*, 6055.
[145] N. Balke, S. Choudhury, S. Jesse, M. Huijben, Y. H. Chu, A. P. Baddorf, L. Q. Chen, R. Ramesh, S. V. Kalinin, *Nat. Nanotechnol.* **2009**, *4*, 868.